



Coencapsulation of disulfiram and doxorubicin in liposomes strongly reverses multidrug resistance in breast cancer cells

Francesca Rolle, Valeria Bincoletto, Elena Gazzano, Barbara Rolando, Giovanna Lollo, Barbara Stella, Chiara Riganti, Silvia Arpicco

► To cite this version:

Francesca Rolle, Valeria Bincoletto, Elena Gazzano, Barbara Rolando, Giovanna Lollo, et al.. Coencapsulation of disulfiram and doxorubicin in liposomes strongly reverses multidrug resistance in breast cancer cells. International Journal of Pharmaceutics, 2020, 580, pp.119191. 10.1016/j.ijpharm.2020.119191 . hal-02498380

HAL Id: hal-02498380

<https://hal.science/hal-02498380>

Submitted on 15 Jan 2024

HAL is a multi-disciplinary open access archive for the deposit and dissemination of scientific research documents, whether they are published or not. The documents may come from teaching and research institutions in France or abroad, or from public or private research centers.

L'archive ouverte pluridisciplinaire **HAL**, est destinée au dépôt et à la diffusion de documents scientifiques de niveau recherche, publiés ou non, émanant des établissements d'enseignement et de recherche français ou étrangers, des laboratoires publics ou privés.

AperTO - Archivio Istituzionale Open Access dell'Università di Torino

Coencapsulation of disulfiram and doxorubicin in liposomes strongly reverses multidrug resistance in breast cancer cells

This is the author's manuscript

Original Citation:

Availability:

This version is available <http://hdl.handle.net/2318/1747153> since 2020-07-29T23:28:28Z

Published version:

DOI:10.1016/j.ijpharm.2020.119191

Terms of use:

Open Access

Anyone can freely access the full text of works made available as "Open Access". Works made available under a Creative Commons license can be used according to the terms and conditions of said license. Use of all other works requires consent of the right holder (author or publisher) if not exempted from copyright protection by the applicable law.

(Article begins on next page)

Manuscript Number:

Title: Coencapsulation of disulfiram and doxorubicin in liposomes
strongly reverses multidrug resistance in breast cancer cells

Article Type: Research Paper

Section/Category: Pharmaceutical Nanotechnology

Keywords: multidrug resistance, P-glycoprotein, liposomes, doxorubicin,
disulfiram, coencapsulation.

Corresponding Author: Professor Silvia Arpicco,

Corresponding Author's Institution: University of Turin

First Author: Francesca Rolle

Order of Authors: Francesca Rolle; Valeria Bincoletto; Elena Gazzano;
Barbara Rolando; Giovanna Lollo; Barbara Stella; Chiara Riganti; Silvia
Arpicco

Abstract: Disulfiram (DSF) is an inhibitor of P-glycoprotein (Pgp), the main obstacle limiting the success of doxorubicin (DOX), but it has poor solubility and stability. With the aim to overcome these limitations we prepared liposomes coencapsulating DSF and DOX (LipoDSF-DOX). Liposome stability, drugs release profile, effects on DOX cytotoxicity, Pgp activity and expression in breast cancer cells were evaluated. We observed that LipoDSF-DOX with a 1:3 weight ratio, with DSF in lipid bilayer and DOX in aqueous core, released DSF faster than DOX. LipoDSF-DOX increased DOX intracellular accumulation and cytotoxicity in Pgp-expressing breast cancer cells, with an efficacy superior to the mixture of free DSF and DOX, thanks to a differential kinetics of release of DSF and DOX when carried by liposomes. The mechanism of the increased DOX retention relied on the DSF-induced sulfhydrylation of Pgp and followed by its ubiquitination. These events reduced Pgp expression and catalytic activity in LipoDSF-DOX-treated cells. Our results show that LipoDSF-DOX effectively reversed DOX resistance in Pgp-expressing breast cancer cells, exploiting the temporally different kinetics of release of DSF and DOX, optimized to decrease expression and activity of Pgp.

Suggested Reviewers: Catherine Passirani
University of Angers / INSERM
catherine.passirani@univ-angers.fr
Expertise in drug delivery and NanoSystems

Helena Oliveira
University of Aveiro, Portugal
holiveira@ua.pt
Expertise on the evolution of in vitro activity of nanoparticles

Radka Vaclavikova Vaclavikova

National Institute of Public Health, Czech Republic
RVaclavikova@seznam.cz
Expertise in MDR

Liliane Massade
IGR, UMR 8203 CNRS
liliane.massade@gustaveroussy.fr
Expertise in the evaluation of the anticancer activity of nanosystems



Via Pietro Giuria, 9
10125 Torino
Tel: +39 011 670.7175
Fax: +39 011 670.7162
e-mail: direzione.farmaco@unito.it

Torino, 25/9/2019

To the kind attention of
Prof. Jürgen Siepmann
Editor-in-Chief

Dear Professor Siepmann,

we are pleased to submit our manuscript entitled **“Coencapsulation of disulfiram and doxorubicin in liposomes strongly reverses multidrug resistance in breast cancer cells”** as original article to International Journal of Pharmaceutics.

Doxorubicin (DOX) is one of the most active and widely used anticancer drugs in the treatment of triple negative breast cancer, but the main limitation to its therapeutic efficacy is the development of multidrug resistance (MDR), mainly due to the overexpression of the efflux transporter P-glycoprotein (Pgp). Pgp is considered an undruggable protein.

Starting from preliminary observations indicating that the anti-alcohol drug disulfiram (DSF, Antabuse[®]) inhibits Pgp, in this work we addressed the challenges of i) improving the poor water solubility and high instability of DSF; ii) coencapsulating DSF and DOX into liposomes, using biocompatible carriers able to improve DSF solubility, and increase DSF and DOX delivery within Pgp-expressing triple negative breast cancer cells. We produced a liposomal formulation with a different and controlled kinetic of release of DSF and DOX: this feature allows a strong inhibition of Pgp by DSF, followed by an increased retention and cytotoxicity exerted by DOX despite the

presence of Pgp. We unveiled the biochemical mechanisms by which DSF reduces activity and expression of Pgp.

Our formulations are the first liposomes coencapsulating DSF and DOX, and had a superior efficacy compared to commercially available/clinically approved liposomal DOX (Caelyx[®] or Doxil[®]).

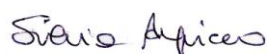
Our results are important in a translational perspective since DOX is the first line-drug in triple-negative breast cancer, *i.e.* the most aggressive form of breast cancer that often expresses Pgp. The results of our work may prioritize the use of liposomes coencapsulating DSF and DOX to improve the current DOX-based treatment of triple-negative breast cancers.

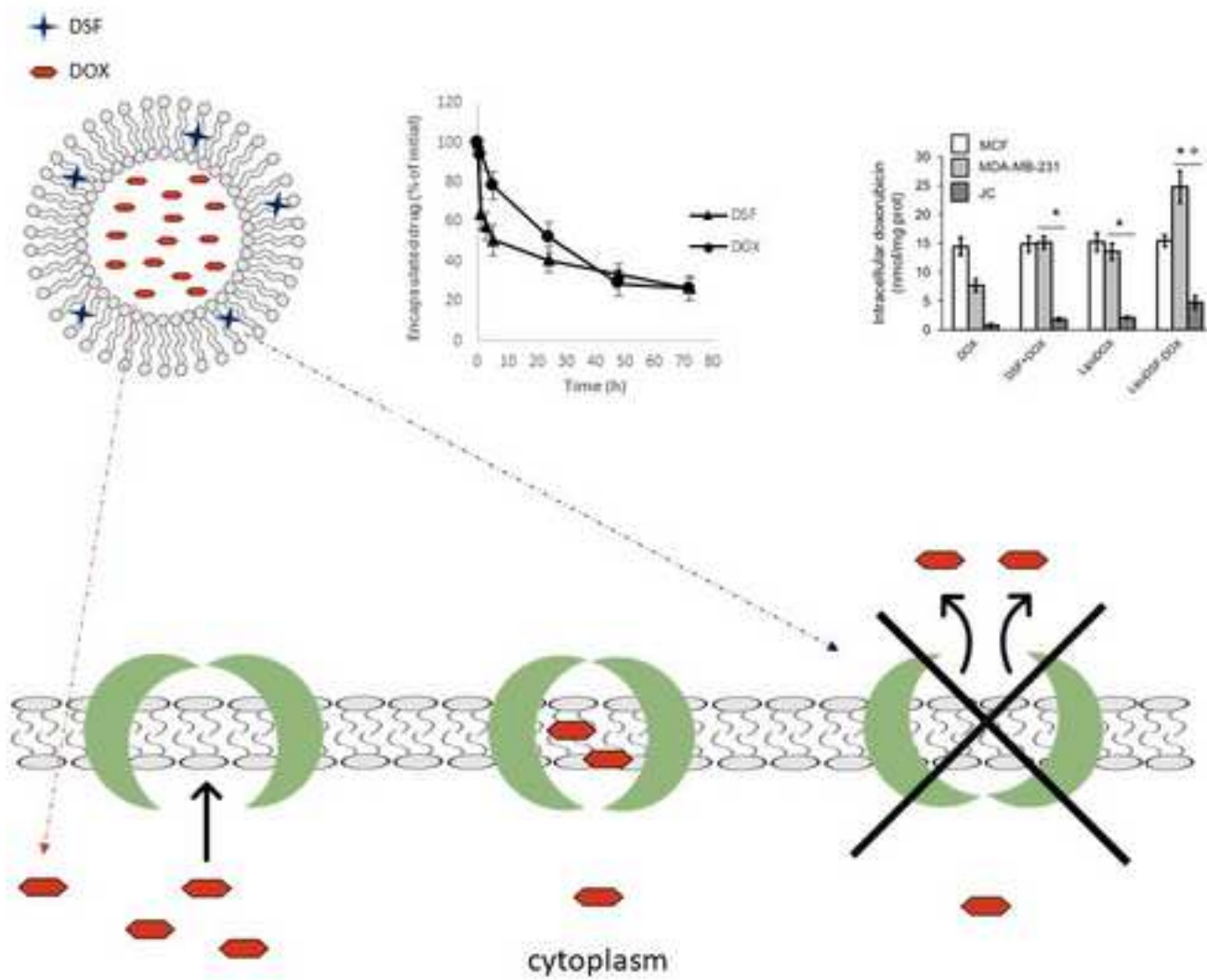
The material is an original research. The manuscript has not been published previously and is not being considered concurrently by another journal.

Authors declare that there are no conflicts of interest.

Sincerely yours,

Silvia Arpicco





**Coencapsulation of disulfiram and doxorubicin in liposomes strongly reverses multidrug
resistance in breast cancer cells**

Francesca Rolle^a, Valeria Bincoletto^a, Elena Gazzano^b, Barbara Rolando^a, Giovanna Lollo^c, Barbara Stella^a, Chiara Riganti^{*,b}, Silvia Arpicco^{*,a}

^a Department of Drug Science and Technology, University of Torino, Via Giuria 9, 10125 Torino, Italy

^b Department of Oncology, University of Torino, via Santena 5/bis, 10126, Torino, Italy

^c CNRS, LAGEPP UMR 5007, University of Lyon, Université Claude Bernard Lyon 1, 43 bd 11 Novembre 1918, 69622, Villeurbanne, France

Corresponding authors Dr. Chiara Riganti, Department of Oncology, University of Torino, via Santena 5/bis, 10126 Torino, Italy; phone: +39116705857; fax: +39116705845; email: chiara.riganti@unito.it; Dr. Silvia Arpicco, Department of Drug Science and Technology, University of Torino, via Pietro Giuria 9, 10125 Torino, Italy; phone: +39116706668; email: silvia.arpicco@unito.it

Abstract

Disulfiram (DSF) is an inhibitor of P-glycoprotein (Pgp), the main obstacle limiting the success of doxorubicin (DOX), but it has poor solubility and stability. With the aim to overcome these limitations we prepared liposomes coencapsulating DSF and DOX (LipoDSF-DOX). Liposome stability, drugs release profile, effects on DOX cytotoxicity, Pgp activity and expression in breast cancer cells were evaluated. We observed that LipoDSF-DOX with a 1:3 weight ratio, with DSF in lipid bilayer and DOX in aqueous core, released DSF faster than DOX. LipoDSF-DOX increased DOX intracellular accumulation and cytotoxicity in Pgp-expressing breast cancer cells, with an efficacy superior to the mixture of free DSF and DOX, thanks to a differential kinetics of release of DSF and DOX when carried by liposomes. The mechanism of the increased DOX retention relied on the DSF-induced sulfhydrylation of Pgp and followed by its ubiquitination. These events reduced Pgp expression and catalytic activity in LipoDSF-DOX-treated cells.

Our results show that LipoDSF-DOX effectively reversed DOX resistance in Pgp-expressing breast cancer cells, exploiting the temporally different kinetics of release of DSF and DOX, optimized to decrease expression and activity of Pgp.

Key words: multidrug resistance, P-glycoprotein, liposomes, doxorubicin, disulfiram, coencapsulation.

1. Introduction

Doxorubicin (DOX) is one of the most active and widely used anticancer drugs in the treatment of early stage and advanced breast cancer. DOX inhibits DNA and RNA synthesis by intercalating between base pairs of the DNA/RNA strand, creates iron-mediated free oxygen radicals, damages the DNA and cell membranes and inhibits topoisomerase II (Minotti et al., 2004). However, DOX possesses two important limitations that hamper its effectiveness: the development of multidrug resistance (MDR) (Gottesman et al., 2002) and the risk of developing cardiac toxicity (Mao et al., 2019).

The most recognized resistance mechanism is the overexpression of P-glycoprotein (Pgp), an ATP binding cassette (ABC) transporters, in the tumor cell plasma-membrane. Pgp effluxes many chemotherapeutic drugs, such as DOX, paclitaxel, docetaxel, vincristine and etoposide, limiting their intracellular accumulation and consequent cytotoxicity.

The commercially available anti-alcohol drug disulfiram (DSF, Antabuse[®]) has shown pharmacological activity as adjuvant tool against Pgp-expressing cells. Micromolar concentrations of DSF act as non competitive inhibitor of Pgp, likely by interacting with cysteines 431 and 1074. Besides reducing the pump's catalytic activity, such modification impairs the complete maturation of the protein, increasing the amount of immature 150 kDa-form over the fully-active and mature 170 kDa form (Loo and Clarke, 2000). The mechanism underlying this inhibition is the covalent binding of cysteine 1074, located in nucleotide binding domain 2 of Pgp, by the DSF metabolites S-methyl N,N-diethylthiocarbamate sulfoxide and S-methyl N,N-diethylthiocarbamate sulfone metabolites generated intracellularly (Loo et al., 2004). From these first experiments, the interest of DSF as potential sensitizer when co-administered with chemotherapeutic drugs that are Pgp substrates as DOX.

The main drawbacks of DSF are its poor water solubility and its high instability (Johansson, 1992). An efficient encapsulation of DSF in nanocarriers such as liposomes could be a strategy to improve

its solubility, to protect it from degradation and to increase its bioavailability. Of note, liposomes carrying DOX determine a higher drug delivery and cytotoxicity against Pgp-expressing cells *in vitro* (Kopecka et al., 2014; Riganti et al., 2011), but liposomal DOX (commercially available as Caelyx[®] or Doxil[®]) was not effective against Pgp-positive tumors *in vivo* (Ma and Mumper, 2013). Liposomes are widely used since they are composed of phospholipids, and thus much more biocompatible than other nanocarriers. Moreover, they can encapsulate a wide range of molecules with hydrophilic, amphiphilic, or lipophilic characteristics (Allen and Cullis, 2013). Until now, some examples of liposomes coencapsulating two different drugs are present in literature: these formulations combine drugs with different physico-chemical properties without altering the concentration of each drug, thus enhancing their colocalization to cancer cells and improving their pharmacodynamics and pharmacokinetics properties (Mu et al., 2017). Very recently a liposomal formulation of daunorubicin and cytarabine in a fixed combination (Vyxeos[™]) has been approved for the treatment of acute myeloid leukemia (Krauss et al., 2019).

With the aim of overcoming the limitations of DSF as free drug and liposomal DOX, we designed and validated liposomes able to co-deliver DSF and DOX as effective tools to increase DOX efficacy against Pgp-positive cells. DSF and DOX were coencapsulated in pegylated liposomes in a precise drug ratio; the lipophilic drug DSF was incorporated into liposomes' bilayer while the hydrophilic drug DOX was encapsulated into the inner core of liposomes. The liposomes were fully characterized and their activity was evaluated *in vitro* against Pgp-positive breast cancer cells to assess if and by which mechanisms these formulations overcome the resistance to DOX induced by Pgp.

2. Materials and methods

2.1 Materials

Fetal bovine serum (FBS) and culture medium were from Invitrogen Life Technologies (Carlsbad, CA). Plasticware for cell cultures was from Falcon (Becton Dickinson, Franklin Lakes, NJ). The protein content in cell extracts was assessed with the BCA kit from Sigma Chemical Co. (St. Louis, MO). Electrophoresis reagents were obtained from Bio-Rad Laboratories (Hercules, CA). Unless otherwise specified, all the other reagents were purchased from Sigma Chemical Co.

2.2 Liposomes preparation and characterization

A new liposomal formulation coencapsulating DSF and DOX (LipoDSF-DOX) was developed. Initially, DSF containing liposomes were prepared using the thin lipid film-hydration method by adding DSF to the lipid mixture to encapsulate the drug into liposomes bilayer; DOX was then encapsulated in the inner aqueous core of DSF containing liposomes by remote loading.

Practically, liposomes containing DSF were obtained by mixing together chloroform solutions of the lipid components (Avanti Polar-Lipids distributed by Sigma- Chemical Co) 1,2-distearoil-*sn*-glycero-3-phosphocoline (DSPC), cholesterol (CHOL) and 1,2-distearoyl-*sn*-glycero-3-phosphoethanolamine-N-[amino(polyethylene glycol)-2000] (mPEG2000-DSPE) in 55:40:5 molar ratio. DSF (Sigma Chemical Co) was added to the lipid mixture in 20% ratio (mol drug/mol lipid). The solution was evaporated and the resulting thin lipid film was dried under vacuum overnight. Lipid film was hydrated with 900 μ l of citric acid buffer (100 mM, pH 4.5) and the suspension was vortex mixed and bath sonicated (20-minute cycle 200 W Powersonic 603 Hwashin Technology Company). Gel filtration using Sepharose CL-4B columns, eluting with HEPES [4-(2-hydroxyethyl) piperazine-1-ethanesulfonic acid] buffer (20 mM, pH 7.4) at room temperature was used to purify liposomes from un-encapsulated DSF and to change the external buffer. To encapsulate DOX into DSF containing liposomes, a solution of DOX hydrochloride (0.1 mg/100 μ l in HEPES buffer) was added to liposomes and incubated at 45 °C for 20 minutes with moderate stirring. The formulation was then extruded (Extruder, Lipex, Vancouver, Canada) at 60 °C under nitrogen through 200 nm polycarbonate membrane (Costar, Corning Incorporated, NY) and un-

encapsulated DOX was removed by gel filtration as previously reported. Liposomes were stored at 4 °C.

For comparison liposomes encapsulating DSF alone (LipoDSF) and DOX alone (LipoDOX) were also prepared.

The mean particle size and the polydispersity index (PI) of liposomes were determined at 25 °C by quasi-elastic light scattering (QELS) using a nanosizer (Nanosizer Nano Z, Malvern Inst., Malvern, UK). The selected angle was 173° and the measurement was made after dilution of the liposomes suspension in MilliQ[®] water. Each measure was performed in triplicate.

The particle surface charge of liposomes was investigated by zeta potential measurements at 25 °C applying the Smoluchowski equation and using the Nanosizer Nano Z. Measurements were carried out in triplicate.

Phospholipid phosphorous was assessed in each liposome preparation by phosphate assay after destruction with perchloric acid (Bartlett, 1959).

The amount of DSF and DOX incorporated in liposomes was determined by reverse phase-high performance liquid chromatography (RP-HPLC). The liposomal formulation was diluted with CH₃CN/water mixture 50/50 v/v, acidified by 0.1% TFA, sonicated, vortexed, and filtered through 0.45 µm PTFE filters (Alltech). The RP-HPLC analysis was performed with a HP 1200 chromatograph system (Agilent Technologies, Palo Alto, CA) equipped with an injector (Rheodyne, Cotati, CA), a quaternary pump (model G1311A), a membrane degasser (model G1322A), a multiple wavelength UV detector (MWD, model G1365D) and a fluorescence detector (FL, model G1321A) integrated in the HP1200 system. The data were processed using a HP ChemStation system (Agilent Technologies). The analytical column was a Zorbax Eclipse XDB-C18 (150 × 4.6 mm, 5 µm; Agilent); the mobile phase consisted of CH₃CN 0.1% TFA (solvent A) and water 0.1% TFA (solvent B) at flow-rate of 1 ml/min with gradient conditions: 35% A until 5 min, from 35 to 80% A between 5 and 10 min, 80% A between 10 and 15 min, and from 80 to 35% A between 15 and 20 min. The injection volume was 20 µl (Rheodyne, Cotati, CA). The column


effluent was monitored at 220 and 234 nm referenced against 800 nm wavelength for DSF, at 480 nm referenced against a 800 nm and in fluorescence (excitation and emission wavelength of 480 and 560 nm respectively, gain factor = 10) for DOX. The quantification of DSF and DOX was done using calibration curves obtained with standard solutions chromatographed in the same experimental conditions, with a concentration range of 1–200 μM ($r^2 > 0.99$).

To evaluate the drug release the formulations were incubated at 37 °C in HEPES buffer for various periods of time and drug leakage was determined submitting 200 μL of liposomes to purification through chromatography on Sepharose CL-4B columns, eluting with HEPES buffer. Then, the drug and lipid content was measured in the collected liposomal fractions and compared with initial values.

The physical stability of liposomes in the storage conditions (4 °C) was determined evaluating at different interval times diameter, zeta potential and drug leakage.

The liposomes morphology was determined by Cryogenic-transmission electron microscopy (cryo-TEM) analysis. The diluted samples were dropped onto 300 Mesh holey carbon films (Quantifoil R2/1) and quench-frozen in liquid ethane using a cryo-plunge workstation (made at LPS Orsay). The specimens were then mounted on a precooled Gatan 62 specimen holder, transferred in the microscope (Phillips CM120) and observed at an accelerating voltage of 120 kV (Centre Technologique des Microstructures (CT μ), platform of the Université Claude Bernard Lyon 1, Villeurbanne, France).

2.3 Cell cultures

Human breast cancer MCF7 cells, human triple negative breast cancer MDA-MB-231 cells, murine triple negative mammary JC cells were purchased from ATCC (Manassas, VA). Cells were cultured in RPMI-1640 medium (Invitrogen, Milan, Italy), supplemented with 10% v/v FBS, 1% v/v penicillin-streptomycin, 1% v/v L-glutamine and maintained in a humidified atmosphere at 37°C. 

2.4 DOX accumulation

DOX content was measured fluorimetrically as detailed elsewhere (Gazzano et al., 2018). Briefly, cells were washed twice with PBS, detached with scraper and centrifuged at 13,000 x g for 5 min at 4 °C. Cell pellets were resuspended in 400 µl of a 1:1 mixture of ethanol/0.3 N HCl and sonicated (1 × 10 s, amplitude 40%; Hielscher UP200S ultrasound sonicator, GmbH, Teltow, Germany). The protein content of cell pellets was assessed with the BCA kit from Sigma Chemicals Co. (St. Louis, MO). The amount of intracellular doxorubicin was detected using a Synergy HT Multi-Detection Microplate Reader (Bio-Tek Instruments, Winoosky, VT). Excitation and emission wavelengths were 475 and 553 nm, respectively. A blank was prepared in the absence of cells in each set of experiments and its fluorescence was subtracted from that measured in each sample. Fluorescence was converted in nmol doxorubicin/mg cell proteins using a protein calibration curve.

2.5 Cell cytotoxicity

The extracellular release of lactate dehydrogenase (LDH), considered an index of cell damage and necrosis, was measured as reported in (Gazzano et al., 2018). The results were expressed as percentage of extracellular LDH versus total (intracellular plus extracellular) LDH. Cell viability was measured by the ATPlite Luminescence Assay System (PerkinElmer, Waltham, MA), as per manufacturer's instructions, using a Synergy HT Multi-Detection Microplate Reader to measure the relative luminescence units (RLU). The RLUs of untreated cells was considered as 100% viability; the results were expressed as a percentage of viable cells *versus* untreated cells.

2.6 Immunoblotting

Cells were rinsed with ice-cold lysis buffer (50 mM Tris, 10 mM EDTA, 1% v/v Triton-X100; pH 7.5), supplemented with the protease inhibitor cocktail set III (80 µM aprotinin, 5 mM bestatin, 1.5 mM leupeptin, 1 mM pepstatin; Calbiochem, San Diego, CA), 2 mM phenylmethylsulfonyl fluoride, 1 mM Na₃VO₄. Cells were then sonicated (10 bursts of 10 sec, 4 °C, 100 W, using a

Labsonic sonicator, Hielscher, Teltow, Germany) and centrifuged at 13,000 x g for 10 min at 4 °C. 20 µg of protein extracts were subjected to 4-20% gradient SDS-PAGE and probed with the following antibodies: anti-ABCB1/Pgp (1:500, Calbiochem, La Jolla, CA); anti ABCC1/Multidrug Resistance Protein 1 (MRP1; 1:100, Abcam, Cambridge, UK); anti-ABCG2/Breast Cancer Resistance protein (BCRP; 1:500, Santa Cruz Biotechnology Inc., Santa Cruz, CA); anti-β-tubulin (1:1,000, Santa Cruz Biotechnology Inc.). To measure ubiquitinated Pgp, 100 µg of whole cell extract proteins were immunoprecipitated with the anti-Pgp antibody, using 25 µl of PureProteome Magnetic Beads (Millipore), then probed with the anti-mono/poly-ubiquitin antibody (1:1,000; Axxora, Lausanne, Switzerland). Plasma membrane-associated proteins were evaluated in biotinylation assays (Salaroglio et al., 2018), and probed with an anti-Pgp or an anti-pancadherin (1:500; Santa Cruz Biotechnology Inc.) antibody. The membranes were then incubated with peroxidase-conjugated secondary antibodies (1:3,000, Bio-Rad Laboratories) and washed with Tris-buffered saline-Tween 0.1% v/v solutions. Protein bands were detected by enhanced chemiluminescence (Bio-Rad Laboratories).

2.7 Pgp activity, sulfhydrylation and ubiquitination assay

The Pgp ATPase activity was measured in Pgp-rich membrane vesicles as described in (Kopecka et al., 2014). The sulfhydrylation of 50 µg of immunopurified Pgp was measured according to (Sen et al., 2012), the ubiquitination was measured with the E3Lite Customizable Ubiquitin Ligase kit (Life-Sensors Inc., Malvern, PA), as detailed elsewhere (Buondonno et al., 2019).

2.8 Statistical analysis

All data in the text and figures are provided as means ± SD. The results were analysed by a one-way analysis of variance (ANOVA) and Tukey's test. $p < 0.05$ was considered significant.

3. Results

3.1 Liposomes preparation and characterization

To obtain a dual drug delivery system for the co-delivery of both DSF and DOX a new pegylated liposomal formulation (LipoDSF-DOX) was developed. In this formulation the lipophilic drug DSF was encapsulated in the lipid bilayer membrane and hydrophilic drug DOX into inner aqueous compartment of liposomes. Different preparation methods, phospholipidic mixtures and drug to phospholipid mole ratios were tested in order to obtain the suitable formulation for further investigations. LipoDSF-DOX was characterized by DSF/DOX weight ratio of 1:3 and the entrapment efficiency value (ratio between drug/lipid molar ratio after purification and drug/lipid molar ratio after extrusion) was around 70% for DSF and 96% for DOX.

The physico-chemical characteristics of LipoDSF-DOX and of liposomes containing the single drug (LipoDSF and LipoDOX) are summarized in Table 1. All liposomes showed a diameter around 120 nm with a low polydispersity index (<0.18) and a similar zeta potential value (around -9 mV).

The release profile of DSF and DOX from LipoDSF-DOX was evaluated in HEPES buffer at 37 °C by removing aliquots of liposomes at different time intervals and re-evaluating drug and phospholipid content after purification. As shown in Figure 1, DSF encapsulated in the liposomal bilayer was released faster (50% after 5 h) than DOX that was precipitated in the inner aqueous core (50% after about 24 h).

Liposomes stability in storage conditions (HEPES buffer at 4 °C) showed that after 21 days they still conserved 85% of the initial drug content and over this period no appreciable size change ($<10\%$ for all the preparations) and no precipitation or liposomes aggregation were observed. Similarly, the zeta potential remained unchanged for the same time period.

Cryo-TEM analysis was used to observe the native structure of liposomes in thin vitrified ice and provide a true snapshot of LipoDSF-DOX (Figure 2). Liposomes appeared unilamellar with both

spherical and elongated shape and DOX precipitated inside the aqueous core of liposomes is visible in most of the vesicles. Their size were consistent with those measured by dynamic light scattering.

3.2 DSF-DOX coencapsulated into liposomes overcome Pgp-mediated resistance to DOX

We compared LipoDSF-DOX with 1:3 weight ratio (corresponding to 3.1 μ M DSF and 5 μ M DOX), with free DOX, DSF + DOX mix at 1:3 weight ratio and LipoDOX in human and murine breast cancer cells with undetectable level of Pgp (*i.e.* MCF7 cells) or constitutively high levels of Pgp (*i.e.* MDA-MB-231 and JC cells) (**Figure 3A**). MRP1 and BCRP, other two transporters involved in DOX efflux were expressed at very low levels (**Figure 3A**), suggesting that they have a minor role in DOX transport in these cells. As expected, Pgp-negative MCF7 accumulated higher amount of DOX than Pgp-positive MDA-MB-231 and JC cells, and DOX content was not modified if the drug was co-incubated with DSF or carried by liposomes, either alone or coencapsulated with DSF (**Figure 3B**). According to the different levels of Pgp, JC cells retained less DOX than MDA-MB-231 and MCF7 cells. In Pgp-positive cells, however, the intracellular accumulation of the drug was significantly increased when DOX was associated with DSF as free drug, incapsulated within liposomes alone or coencapsulated with DSF (**Figure 3B**). LipoDSF-DOX was the formulation that produced the highest accumulation of DOX compared to DSF+DOX or LipoDOX (**Figure 3B**), and with LipoDSF-DOX with other weight ratios (data not shown).

Consistently, DOX induced acute cell damage, measured as extracellular release of LDH, and reduced cell viability in MCF7 cells (**Figure 3C**), but not in MDA-MB-231 (**Figure 3D**) and JC (**Figure 3E**) cells. In Pgp-negative cells, DSF did not increase DOX cytotoxic effects (**Figure 3C**), while it did so in Pgp-positive cells (**Figure 3D-E**). Again, LipoDSF-DOX was more cytotoxic than the mix of free drugs DSF + DOX or LipoDOX in both MDA-MB-231 (**Figure 3D**) and JC (**Figure 3E**) cells. No cytotoxicity was exerted by LipoDSF, suggesting that DSF was devoid of toxicity in the experimental conditions adopted (**Figure 3C-E**).

We then investigated the mechanisms underlying of the higher efficacy of LipoDSF-DOX in Pgp-positive cells.

3.3 DSF-DOX coencapsulated into liposomes reduced Pgp activity and expression

DSF, alone, associated with DOX as free drug or coencapsulated in liposomes, reduced the Pgp ATPase activity in MDA-MB-231 and JC cells, while DOX had no effect (**Figure 4A**). The reduction in Pgp activity was paralleled by increased sulfhydrylation (**Figure 4B**) and ubiquitination of Pgp, as demonstrated by a chemiluminescence-based assay (**Figure 4C**) and by the detection of ubiquitinated Pgp after its immunoprecipitation (**Figure 4D**), in all the cells treated with DSF. Consequently, the amount of Pgp present in whole cell lysate (**Figure 4D**), *i.e.* the total Pgp, and on cell surface, *i.e.* the active form of the protein, was lower after exposure to DSF, DSF+DOX or LipoDSF-DOX (**Figure 4E**).

4. Discussion

DOX and liposomal DOX are widely used in cancer treatment, but their clinical effectiveness is dramatically decreased by the presence of Pgp. Several pharmacological agents have been proposed as inhibitors of Pgp, including calcium channel blockers, immunosuppressive agents, quinolones: although effective *in vitro*, they lacked of efficacy *in vivo* because of their poor specificity and high toxicity (Callaghan et al., 2014).

An alternative strategy to overcome MDR is to coencapsulate a Pgp inhibitor and an anticancer drug in a nanovector to deliver and release the two components in a controlled release manner and suitable ratio, thus improving the therapeutic potential (Jose et al., 2019; Li et al., 2019; Tang et al., 2016).

Here we developed a novel liposomal formulation to codeliver DSF and DOX at the optimal weight ratio with higher antitumor activity on drug-resistant cancer cells in comparison to DOX either

alone or encapsulated in liposomes. DSF was encapsulated in liposomes bilayer by rehydration of the thin lipid in a low pH citrate buffer that allows both to reduce the instability of DSF (Chen et al., 2015) and to obtain a pH gradient mediated DOX loading that precipitates inside liposomes aqueous core as citrate salt (Swenson et al., 2001) in the typical road like precipitate structure observed by others for DOX liposomal formulations (Fritze et al., 2006). Moreover, it has been demonstrated that DSF strongly interacts through hydrophobic interactions with the liposome bilayer (Marengo et al., 2019).

All these data show that the proposed preparation method allowed to obtain the dual drug loaded liposomes with controlled drug ratio. LipoDSF-DOX showed an interesting and useful controlled release profile: DSF was released faster than DOX. This kinetic profile led us to hypothesize that free DSF or its metabolites produced intracellularly were able to inhibit Pgp activity, allowing the higher accumulation of DOX coencapsulated in the same liposomes and released with a slower kinetics. Indeed, in our experimental conditions, DSF increased the intracellular retention of DOX either as free drug or when coencapsulated within liposomes, with higher efficacy when used as LipoDSF-DOX. The higher efficacy of the liposomal formulation compared to the DSF + DOX mix can be explained by the temporally different kinetics of release of DSF and DOX when they are delivered by liposomes.

Our work is in line with previous observations reporting that the coencapsulation of DOX with DSF improved the efficacy of the former against breast cancer cells. For instance, polymeric micelles coencapsulating DSF and DOX increased the DOX delivery within Pgp-positive MCF7/ADR cells, not within parental MCF7 cells (Duan et al., 2013). In partial contrast, core-shell nanoparticles carrying DSF and DOX increased the DOX accumulation either in Pgp-negative MCF7 or in Pgp-positive MDA-MB231 cells (Tao et al., 2018). Of note, while the temporal-controlled release profile of DSF and DOX in the work of Duan was similar to our experimental conditions, in the case of Tao and coworkers the DSF release profile was slower. We were the first group synthesizing liposomal coencapsulating DSF and DOX, with a temporal drug release profile that

maximizes the chemosensitizing effects on Pgp-expressing cells. This effect was not species-specific, as demonstrated by the superior efficacy of LipoDSF-DOX compared to free DOX, mix of free DSF and DOX or LipoDOX in both human and murine Pgp-expressing cancer cells. On the other hand, our formulations were specific for targeting Pgp: indeed they increased the intracellular retention of DOX in MDA-MB-231 and JC cells, where they reduced expression and activity of Pgp, not in MCF7 cells, where Pgp, *i.e.* the putative target of DSF, was undetectable. Since cancer stem cells highly express Pgp (Riganti et al., 2019; Riganti et al., 2013; Wagner-Souza et al., 2008) and are the most chemoresistant tumor cells (Zhao, 2016) this specificity of LipoDSF-DOX for Pgp-expressing cells might be exploited to achieve a better killing of cancer stem cell. Interestingly, a selective toxicity of DSF for stem cells, independent on the effects on Pgp but due to the inhibition of aldehyde dehydrogenase, an enzyme particularly abundant in the stem cell compartment, has been already reported (Liu et al., 2013; MacDonagh et al., 2017). According to these premises, LipoDSF-DOX may be regarded as a promising strategy able to improve the eradication of cancer stem cells and to overcome at the same time the Pgp-associated chemoresistance in this tumor component.

In our conditions, LipoDSF did not induce cell damage nor reduce cell viability when used alone, likely because the encapsulated drug was at 3.1 μM concentration, beyond the range of concentrations ($\geq 10 \mu\text{M}$) used to induce a direct cytotoxic effect in breast cancer cells (Yip et al., 2011). Although obtained *in vitro*, these results suggest that, at this concentration and with this type of formulation, DSF can represent an effective DOX-sensitizing agent against Pgp-expressing breast tumors. We are currently evaluating the best schedule treatment maximizing the therapeutic benefit of LipoDSF-DOX in murine models of breast cancers.

In line with previous observations on free DSF (Loo and Clarke, 2000), also in the case of liposomal formulation the main effect induced in Pgp-expressing cells was the reduction in Pgp catalytic activity. We found that this reduction was paralleled by a significant increase in Pgp sulfhydrylation, a process that impairs the stability of Pgp and induces its ubiquitination (Buondonno

et al., 2019). Pgp has several cysteines whose alterations or mutations alter catalytic cycle, ATP binding and protein stability (Pan and Aller, 2015; Swartz et al., 2014). In the case of DSF metabolites, site-directed mutagenesis approach demonstrated that cysteine 1074 is likely the target of DSF metabolite: following the alkylation of this cysteine, the protein stability is altered and Pgp cannot mature properly (Loo et al., 2004). Differently from this work, we did not find any impairment of maturation of Pgp, because we always found one molecular band of 170 kDa, corresponding to mature Pgp, in our cells. This could be due to the different biological sample (purified Pgp in the work of Loo et al, whole cell lysate in our work), extraction protocol and/or panel of glycosidase and glycosyl transferase present in yeasts, analyzed by Loo, and in mammalian cells, analyzed in the present work. Sulfhydrylation can activate or inhibit protein function. In the case of Pgp, the sulfhydrylation induced by synthetic H₂S-releasing DOX, either as free drug (Buondonno et al., 2019) or liposomal formulation (Gazzano et al., 2019) triggered Pgp ubiquitination, reducing the amount of protein present on cell surface, *i.e.* actively extruding DOX (Buondonno et al., 2019; Gazzano et al., 2019). According to our results, DSF induces the same effects of H₂S-releasing DOX, altering the disulfide bonds of Pgp architecture, protein conformation and stability. As it commonly occurs when unfolded proteins levels increase, the proteins undergo ubiquitination (Chevet et al., 2015). These events occur also upon exposure to DSF. We did not notice any difference between free DSF or liposomal DSF, suggesting that both the kinetics of uptake of free drug or uptake of liposomes and subsequent release of DSF from liposomal shell yield sufficient intracellular DSF (or DSF-related metabolites) to produce an appreciable sulfhydrylation of Pgp. Of note, DSF produced the same effect on Pgp of human and murine origin: since murine Pgp has no cysteine homologue to human cysteine 1074 (Wolffe et al., 1990), it is unlikely that this is the target of sulfhydrylation elicited by DSF. Interesting mouse Pgp have 7 cysteine residues, contained in nucleotide binding domains and transmembrane domains (Wolffe et al., 1990). We hypothesized that sulfhydrylation elicited by DSF or its metabolites targets one or more cysteines present in these domains and homologue between humans and mice, thus

impairing protein stability and catalytic efficiency. As a result, the intracellular retention and cytotoxicity of DOX increased, overcoming the Pgp-mediated resistance.

We cannot exclude that other mechanisms are involved in chemosensitizing cancer cells to DOX if treated with DSF. For instance, DSF synergizes with DOX by activating JNK/c-jun pro-apoptotic pathways (Xu et al., 2011), by interfering with NF- κ B pro-survival signalling (Yip et al., 2011) and by inhibiting IQGAP1 and myosin heavy-chain 9 (MYH9), two hub proteins that stimulate cell cycle and migration (Robinson et al., 2013). Moreover, by selectively depleting cancer-associated stem cells thanks to the inhibition of aldehyde dehydrogenase (MacDonagh et al., 2017; Wu et al., 2019), an enzyme highly expressed in stem cell population, DSF enhanced the cytotoxicity of taxol or cisplatin. Of note, these chemotherapeutic agents are substrates of Pgp. Therein, at least part of the synergistic effect obtained by the combination of DSF and chemotherapy may be due to the reduced drugs efflux through Pgp. This hypothesis is supported by the data obtained in the present work, showing that DSF is effective as chemosensitizer agents in Pgp-positive cells only.

In summary, we propose the proof of concept liposomes coencapsulating DSF and DOX as potent tools able to grant a temporarily controlled release of DSF and a significant inhibition of Pgp activity, overcoming the resistance to DOX mediated by this transporter. Our results are important in a translational perspective since DOX is the first line-drug in triple-negative breast cancer (Harbeck and Gnant, 2017), the most aggressive form of breast cancer and the most frequently chemoresistant (Szekely et al., 2017). Unluckily, triple negative breast cancer cells have often high levels of Pgp (Gazzano et al., 2018; Salaroglio et al., 2018) that limits DOX efficacy. Overcoming DOX resistance is a clinical unmet need in triple-negative breast cancer treatment. If the efficacy of LipoDSF-DOX observed *in vitro* is maintained in animal models, we can reasonably prioritize this approach as an improvement in the current DOX-based treatment of triple-negative breast cancer patients.

Acknowledgements:

We would like to acknowledge the contribution of Pierre-Yves Dugas (University of Lyon 1, C2P2 UMR 5265, France) for cryo-TEM observations at the “Centre Technologique des Microstructures” (CT μ - University of Lyon 1) and Dr. Alessandro Marengo (Department of Drug Science and Technology, University of Torino, Italy) for the fruitful discussions.

Funding sources:

This work was supported by the Italian Association for Cancer Research (AIRC; IG214028) and by Italian Ministry for University and Research (MIUR)—University of Torino, “Fondi Ricerca Locale (ex-60%)”.

References

- Allen, T.M., Cullis, P.R., 2013. Liposomal drug delivery systems: From concept to clinical applications. *Adv Drug Deliver Rev* 65, 36-48.
- Bartlett, G.R., 1959. Phosphorus assay in column chromatography. *J Biol Chem* 234, 466-468.
- Buondonno, I., Gazzano, E., Tavanti, E., Chegaev, K., Kopecka, J., Fanelli, M., Rolando, B., Fruttero, R., Gasco, A., Hattinger, C., Serra, M., Riganti, C., 2019. Endoplasmic reticulum-targeting doxorubicin: a new tool effective against doxorubicin-resistant osteosarcoma. *Cell Mol Life Sci* 76, 609-625.
- Callaghan, R., Luk, F., Bebawy, M., 2014. Inhibition of the Multidrug Resistance P-Glycoprotein: Time for a Change of Strategy? *Drug Metab Dispos* 42, 623-631.
- Chen, X., Zhang, L., Hu, X., Lin, X., Zhang, Y., Tang, X., 2015. Formulation and preparation of a stable intravenous disulfiram-loaded lipid emulsion. *Eur J Lipid Sci Tech* 117, 869-878.
- Chevet, E., Hetz, C., Samali, A., 2015. Endoplasmic reticulum stress-activated cell reprogramming in oncogenesis. *Cancer Discov* 5, 586-597.
- Duan, X.P., Xiao, J.S., Yin, Q., Zhang, Z.W., Yu, H.J., Mao, S.R., Li, Y.P., 2013. Smart pH-Sensitive and Temporal-Controlled Polymeric Micelles for Effective Combination Therapy of Doxorubicin and Disulfiram. *Acs Nano* 7, 5858-5869.
- Fritze, A., Hens, F., Kimpfler, A., Schubert, R., Peschka-Suss, R., 2006. Remote loading of doxorubicin into liposomes driven by a transmembrane phosphate gradient. *Bba-Biomembranes* 1758, 1633-1640.
- Gazzano, E., Buondonno, I., Marengo, A., Rolando, B., Chegaev, K., Kopecka, J., Saponara, S., Sorge, M., Hattinger, C.M., Gasco, A., Fruttero, R., Brancaccio, M., Serra, M., Stella, B., Fattal, E., Arpicco, S., Riganti, C., 2019. Hyaluronated liposomes containing H₂S-releasing doxorubicin are effective against P-glycoprotein-positive/doxorubicin-resistant osteosarcoma cells and xenografts. *Cancer Lett* 456, 29-39.
- Gazzano, E., Rolando, B., Chegaev, K., Salaroglio, I.C., Kopecka, J., Pedrini, I., Saponara, S., Sorge, M., Buondonno, I., Stella, B., Marengo, A., Valoti, M., Brancaccio, M., Fruttero, R., Gasco, A., Arpicco, S., Riganti, C., 2018. Folate-targeted liposomal nitrooxy-doxorubicin: An effective tool against P-glycoprotein-positive and folate receptor-positive tumors. *Journal of Controlled Release* 270, 37-52.
- Gottesman, M.M., Fojo, T., Bates, S.E., 2002. Multidrug resistance in cancer: Role of ATP-dependent transporters. *Nat Rev Cancer* 2, 48-58.
- Harbeck, N., Gnant, M., 2017. Breast cancer. *Lancet* 389, 1134-1150.
- Johansson, B., 1992. A Review of the Pharmacokinetics and Pharmacodynamics of Disulfiram and Its Metabolites. *Acta Psychiat Scand* 86, 15-26.

Jose, A., Ninave, K.M., Karnam, S., Venuganti, V.V.K., 2019. Temperature-sensitive liposomes for co-delivery of tamoxifen and imatinib for synergistic breast cancer treatment. *Journal of Liposome Research* 29, 153-162.

Kopecka, J., Salzano, G., Campia, I., Lusa, S., Ghigo, D., De Rosa, G., Riganti, C., 2014. Insights in the chemical components of liposomes responsible for P-glycoprotein inhibition. *Nanomed-Nanotechnol* 10, 77-87.

Krauss, A.C., Gao, X., Li, L., Manning, M.L., Patel, P., Fu, W.T., Janoria, K.G., Gieser, G., Bateman, D.A., Przepiorka, D., Shen, Y.L., Shord, S.S., Sheth, C.M., Banerjee, A., Liu, J., Goldberg, K.B., Farrell, A.T., Blumenthal, G.M., Pazdur, R., 2019. FDA Approval Summary: (Daunorubicin and Cytarabine) Liposome for Injection for the Treatment of Adults with High-Risk Acute Myeloid Leukemia. *Clin Cancer Res* 25, 2685-2690.

Li, Y., Luo, J., Lin, M.T., Zhi, P., Guo, W.W., You, J., Gao, J.Q., 2019. Co-Delivery of Metformin Enhances the Antimultidrug Resistant Tumor Effect of Doxorubicin by Improving Hypoxic Tumor Microenvironment. *Mol Pharmaceut* 16, 2966-2979.

Liu, P., Kumar, I.S., Brown, S., Kannappan, V., Tawari, P.E., Tang, J.Z., Jiang, W., Armesilla, A.L., Darling, J.L., Wang, W., 2013. Disulfiram targets cancer stem-like cells and reverses resistance and cross-resistance in acquired paclitaxel-resistant triple-negative breast cancer cells. *Brit J Cancer* 109, 1876-1885.

Loo, T.W., Bartlett, M.C., Clarke, D.M., 2004. Disulfiram metabolites permanently inactivate the human multidrug resistance P-glycoprotein. *Mol Pharmaceut* 1, 426-433.

Loo, T.W., Clarke, D.M., 2000. Blockage of drug resistance in vitro by disulfiram, a drug used to treat alcoholism. *Inci-J Natl Cancer I* 92, 898-902.

Ma, P., Mumper, R.J., 2013. Anthracycline nano-delivery systems to overcome multiple drug resistance: A comprehensive review. *Nano Today* 8, 313-331.

MacDonagh, L., Gallagher, M.F., Ffrench, B., Gasch, C., Breen, E., Gray, S.G., Nicholson, S., Leonard, N., Ryan, R., Young, V., O'Leary, J.J., Cuffe, S., Finn, S.P., O'Byrne, K.J., Barr, M.P., 2017. Targeting the cancer stem cell marker, aldehyde dehydrogenase 1, to circumvent cisplatin resistance in NSCLC. *Oncotarget* 8, 72544-72563.

Mao, Z.J., Shen, K.P., Zhu, L.M., Xu, M.D., Yu, F., Xue, D.J., Li, H.G., Xue, C., 2019. Comparisons of Cardiotoxicity and Efficacy of Anthracycline-Based Therapies in Breast Cancer: A Network Meta-Analysis of Randomized Clinical Trials. *Oncol Res Treat* 42, 405-413.

Marengo, A., Forciniti, S., Dando, I., Dalla Pozza, E., Stella, B., Tsapis, N., Yagoubi, N., Fanelli, G., Fattal, E., Heeschen, C., Palmieri, M., Arpicco, S., 2019. Pancreatic cancer stem cell proliferation is strongly inhibited by diethyldithiocarbamate-copper complex loaded into hyaluronic acid decorated liposomes. *Bba-Gen Subjects* 1863, 61-72.

Minotti, G., Menna, P., Salvatorelli, E., Cairo, G., Gianni, L., 2004. Anthracyclines: Molecular advances and pharmacologic developments in antitumor activity and cardiotoxicity. *Pharmacol Rev* 56, 185-229.

Mu, L.M., Ju, R.J., Liu, R., Bu, Y.Z., Zhang, J.Y., Li, X.Q., Zeng, F., Lu, W.L., 2017. Dual-functional drug liposomes in treatment of resistant cancers. *Adv Drug Deliv Rev* 115, 46-56.

Pan, L.R., Aller, S.G., 2015. Equilibrated Atomic Models of Outward-Facing P-glycoprotein and Effect of ATP Binding on Structural Dynamics. *Sci Rep-Uk* 5, 7880.

Riganti, C., Contino, M., Guglielmo, S., Perrone, M.G., Salaroglio, I.C., Milosevic, V., Giampietro, R., Leonetti, F., Rolando, B., Lazzarato, L., Colabufo, N.A., Fruttero, R., 2019. Design, Biological Evaluation, and Molecular Modeling of Tetrahydroisoquinoline Derivatives: Discovery of A Potent P-Glycoprotein Ligand Overcoming Multidrug Resistance in Cancer Stem Cells. *J Med Chem* 62, 974-986.

Riganti, C., Salaroglio, I.C., Caldera, V., Campia, I., Kopecka, J., Mellai, M., Annovazzi, L., Bosia, A., Ghigo, D., Schiffer, D., 2013. Temozolomide downregulates P-glycoprotein expression in glioblastoma stem cells by interfering with the Wnt3a/glycogen synthase-3 kinase/beta-catenin pathway. *Neuro Oncol* 15, 1502-1517.

Riganti, C., Voena, C., Kopecka, J., Corsetto, P.A., Montorfano, G., Enrico, E., Costamagna, C., Rizzo, A.M., Ghigo, D., Bosia, A., 2011. Liposome-Encapsulated Doxorubicin Reverses Drug Resistance by Inhibiting P-Glycoprotein in Human Cancer Cells. *Mol Pharmaceut* 8, 683-700.

Robinson, T.J., Pai, M., Liu, J.C., Vizeacoumar, F., Sun, T., Egan, S.E., Datti, A., Huang, J., Zacksenhaus, E., 2013. High-throughput screen identifies disulfiram as a potential therapeutic for triple-negative breast cancer cells: interaction with IQ motif-containing factors. *Cell Cycle* 12, 3013-3024.

Salaroglio, I.C., Gazzano, E., Abdullrahman, A., Mungo, E., Castella, B., Abd-Elrahman, G.E.F.A., Massaia, M., Donadelli, M., Rubinstein, M., Riganti, C., Kopecka, J., 2018. Increasing intratumor C/EBP- LIP and nitric oxide levels overcome resistance to doxorubicin in triple negative breast cancer. *J Exp Clin Canc Res* 37, 286.

Sen, N., Paul, B.D., Gadalla, M.M., Mustafa, A.K., Sen, T., Xu, R.S., Kim, S., Snyder, S.H., 2012. Hydrogen Sulfide-Linked Sulfhydration of NF-kappa B Mediates Its Antiapoptotic Actions. *Mol Cell* 45, 13-24.

Swartz, D.J., Mok, L., Botta, K., Singh, A., Altenberg, G.A., Urbatsch, I.L., 2014. Directed evolution of P-glycoprotein cysteines reveals site-specific, non-conservative substitutions that preserve multidrug resistance. *Bioscience Rep* 34, 297-U282.

Swenson, C.E., Perkins, W.R., Roberts, P., Janoff, A.S., 2001. Liposome technology and the development of Myocet (TM) (liposomal doxorubicin citrate). *Breast* 10, 1-7.

Szekely, B., Silber, A.L.M., Pusztai, L., 2017. New Therapeutic Strategies for Triple-Negative Breast Cancer. *Oncology-Ny* 31, 13-20.

Tang, J., Zhang, L., Gao, H.L., Liu, Y.Y., Zhang, Q.Y., Ran, R., Zhang, Z.R., He, Q., 2016. Co-delivery of doxorubicin and P-gp inhibitor by a reduction-sensitive liposome to overcome multidrug resistance, enhance anti-tumor efficiency and reduce toxicity. *Drug Deliv* 23, 1130-1143.

Tao, X.G., Gou, J.X., Zhang, Q.Y., Tan, X.Y., Ren, T.Y., Yao, Q., Tian, B., Kou, L.F., Zhang, L., Tang, X., 2018. Synergistic breast tumor cell killing achieved by intracellular co-delivery of doxorubicin and disulfiram via core-shell-corona nanoparticles. *Biomater Sci-Uk* 6, 1869-1881.

Wagner-Souza, K., Diamond, H.R., Ornellas, M.H., Gomes, B.E., Almeida-Oliveira, A., Abdelhay, E., Bouzas, L.F., Rumjanek, V.M., 2008. Rhodamine 123 efflux in human subpopulations of hematopoietic stem cells: Comparison between bone marrow, umbilical cord blood and mobilized peripheral blood CD34(+) cells. *Int J Mol Med* 22, 237-242.

Wolffe, E.J., Gause, W.C., Pelfrey, C.M., Holland, S.M., Steinberg, A.D., August, J.T., 1990. The cDNA sequence of mouse Pgp-1 and homology to human CD44 cell surface antigen and proteoglycan core/link proteins. *J Biol Chem* 265, 341-347.

Wu, L., Meng, F.Y., Dong, L., Block, C.J., Mitchell, A.V., Wu, J., Jang, H., Chen, W., Polin, L., Yang, Q.F., Dou, Q.P., Wu, G.J., 2019. Disulfiram and BKM120 in Combination with Chemotherapy Impede Tumor Progression and Delay Tumor Recurrence in Tumor Initiating Cell-Rich TNBC. *Sci Rep-Uk* 9, 236.

Xu, B., Shi, P., Fombon, I.S., Zhang, Y., Huang, F., Wang, W., Zhou, S., 2011. Disulfiram/copper complex activated JNK/c-jun pathway and sensitized cytotoxicity of doxorubicin in doxorubicin resistant leukemia HL60 cells. *Blood Cells Mol Dis* 47, 264-269.

Yip, N.C., Fombon, I.S., Liu, P., Brown, S., Kannappan, V., Armesilla, A.L., Xu, B., Cassidy, J., Darling, J.L., Wang, W., 2011. Disulfiram modulated ROS-MAPK and NF kappa B pathways and targeted breast cancer cells with cancer stem cell-like properties. *Brit J Cancer* 104, 1564-1574.

Zhao, J.H., 2016. Cancer stem cells and chemoresistance: The smartest survives the raid. *Pharmacol Therapeut* 160, 145-158.

Figure captions:

Figure 1. *In vitro* release profile of DSF and DOX from LipoDSF-DOX.

The results are expressed as percentage of the initial drug remaining in liposomes, at different time periods, and are presented as mean \pm SD (n = 3).

Figure 2: Cryogenic-transmission electron microscopy images of LipoDSF-DOX.

The arrows indicate linear bundle of DOX inside the liposome structure. E represents the enlargement of the liposome captured in D, DOX bundle is present inside the nanostructure.

Figure 3. Effects of DSF-DOX coencapsulated into liposomes in Pgp-expressing breast cancer cells.

Human breast MCF7 and MDA-MB-231 cells and murine mammary cancer JC cells were grown 6 h (DOX accumulation), 24 h (LDH release) or 72 h (viability assay) in fresh medium (Ctrl) or in medium containing 5 μ M DOX, 3.1 μ M DSF and 5 μ M DOX (1:3 weight ratio; DSF+DOX), liposomes containing 5 μ M DOX (LipoDOX), 3.1 μ M DSF (LipoDSF), 3.1 μ M DSF and 5 μ M DOX (1:3 weight ratio; LipoDSF-DOX). **A.** Expression of Pgp, MRP1 and BCRP in untreated cells, measured by immunoblotting. The β -tubulin expression was used as control of equal protein loading. The figure is representative of 1 out of 3 experiments. **B.** Intracellular DOX accumulation, measured by a fluorimetric assay in duplicates. Data are means \pm SD (n=4 independent experiments). *p<0.001: DSF+DOX/LipoDOX/LipoDSF-DOX vs. DOX; °p< 0.001: LipoDSF-DOX vs. DSF+DOX/LipoDOX. **B-D.** Extracellular release of LDH (left panels), measured spectrophotometrically in triplicates, and cell viability (right panels), measured by a chemiluminescence-based assay in quadruplicates. Data are means \pm SD (n=6 independent experiments). *p<0.01: DOX/DSF+DOX/LipoDOX/LipoDSF-DOX vs. respective untreated (Ctrl) cells; °p<0.02: DSF+DOX/LipoDOX/LipoDSF-DOX vs. DOX; #p<0.01: LipoDSF-DOX vs. DSF+DOX/LipoDOX.

Figure 4. Impact of DSF-DOX coencapsulated into liposomes on Pgp activity and expression.

Human breast MDA-MB-231 cells and murine mammary cancer JC cells were grown 24 h in fresh medium (Ctrl) or in medium containing 3.1 μ M disulfiram (DSF or DS), 5 μ M doxorubicin (DOX or D), 3.1 μ M disulfiram and 5 μ M doxorubicin (1:3 weight ratio; DSF+DOX or DS+D), liposomes containing 3.1 μ M disulfiram (LipoDSF or LDS), 5 μ M doxorubicin (LipoDOX or LD), 3.1 μ M disulfiram and 5 μ M doxorubicin (1:3 weight ratio; LipoDSF-DOX or LDS-D). **A.** Pgp ATPase activity was measured spectrophotometrically in triplicates on Pgp isolated by immunoprecipitation from whole cell extracts. Data are means \pm SD (n=4 independent experiments). *p<0.001: DSF/DSF+DOX/LipoDSF/LipoDSF-DOX vs. respective untreated (Ctrl) cells; °p<0.001: DSF+DOX/LipoDSF-DOX vs. DOX. **B.** Pgp was isolated by immunoprecipitation whole cell extracts; the amount of sulfhydrated Pgp was measured fluorimetrically in triplicates. Data are means \pm SD (n=4 independent experiments). *p<0.001: DSF/DSF+DOX/LipoDSF/LipoDSF-DOX vs. respective untreated (Ctrl) cells; °p<0.001: DSF+DOX/LipoDSF-DOX vs. DOX. **C.** Ubiquitinated Pgp, isolated by immunoprecipitation, was measured by a chemiluminescence-based assay in triplicates. Data are means \pm SD (n=4 independent experiments). *p<0.001: DSF/DSF+DOX/LipoDSF/LipoDSF-DOX vs. respective untreated (Ctrl) cells; °p<0.001: DSF+DOX/LipoDSF-DOX vs. DOX. **D.** Microsomal proteins were immunoprecipitated (IP) with an anti-Pgp antibody, then immunoblotted (IB) with an anti-mono/poly-ubiquitin (UQ) antibody. An aliquot of the samples before immunoprecipitation was probed with an anti-Pgp antibody or with an anti-calreticulin antibody, used as control of equal protein loading. no Ab: untreated cell lysate immunoprecipitated in the absence of antibody, to check the specificity of the procedure. MW: molecular weight. The figure is representative of 1 out of 3 experiments. **E.** Expression of Pgp associated to plasma-membrane, isolated by biotinylation assay, evaluated by immunoblotting. The β -tubulin expression was used as control of equal protein loading. The figure is representative of 1 out of 3 experiments.

Declaration of interests

☒ The authors declare that they have no known competing financial interests or personal relationships that could have appeared to influence the work reported in this paper.

☐ The authors declare the following financial interests/personal relationships which may be considered as potential competing interests:

Table 1
Characteristics of liposomal formulations (means \pm SD; n=3).

Formulation	Mean particle size (nm)	Polydispersity index	Zeta potential (mV)
LipoDOX	122 \pm 1	0.131	-7.9 \pm 0.8
LipoDSF	115 \pm 2	0.178	-8.9 \pm 1.1
LipoDSF-DOX	118 \pm 1	0.171	-8.6 \pm 0.5

Figure 1

Figure 1

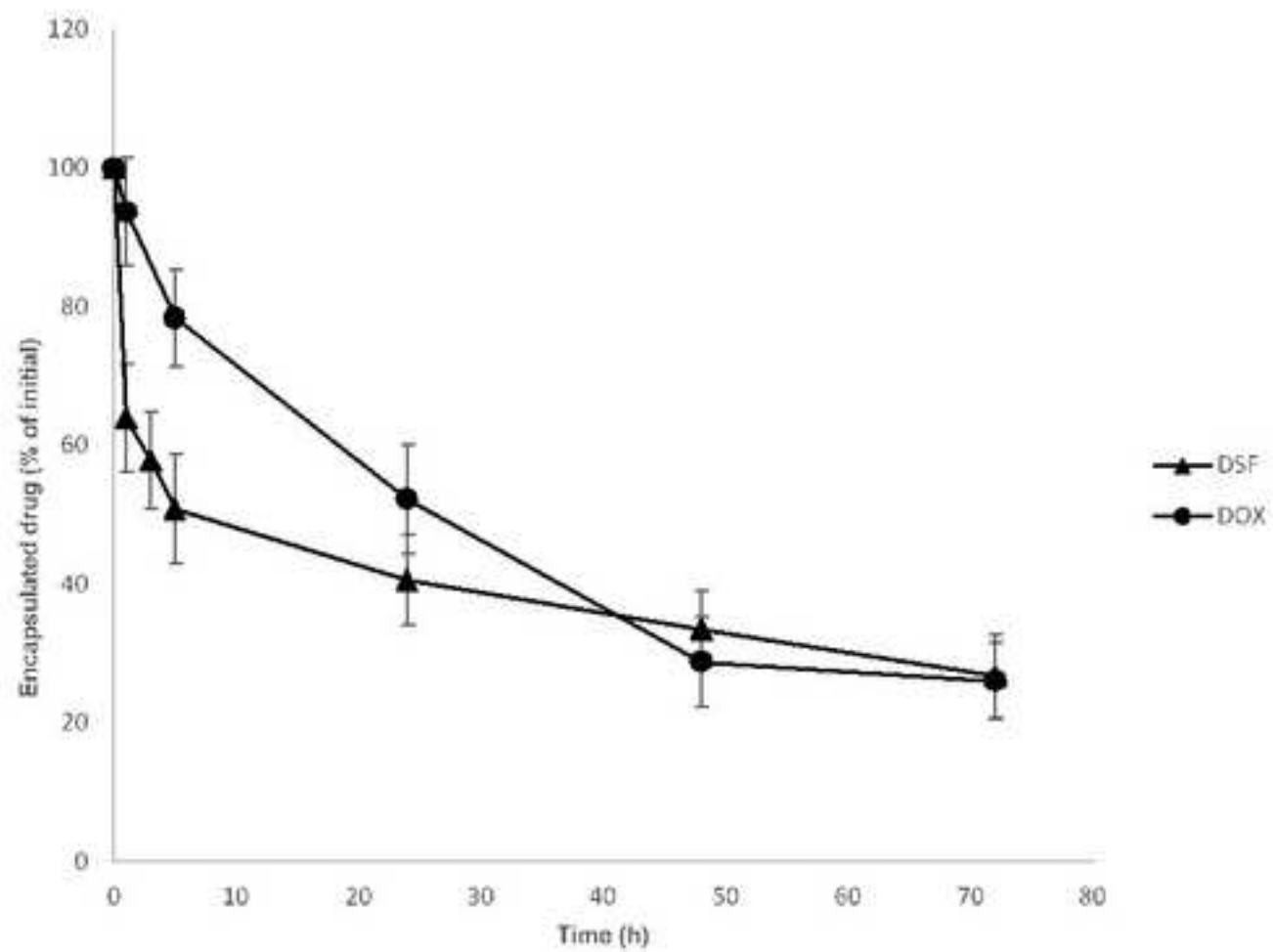


Figure 2

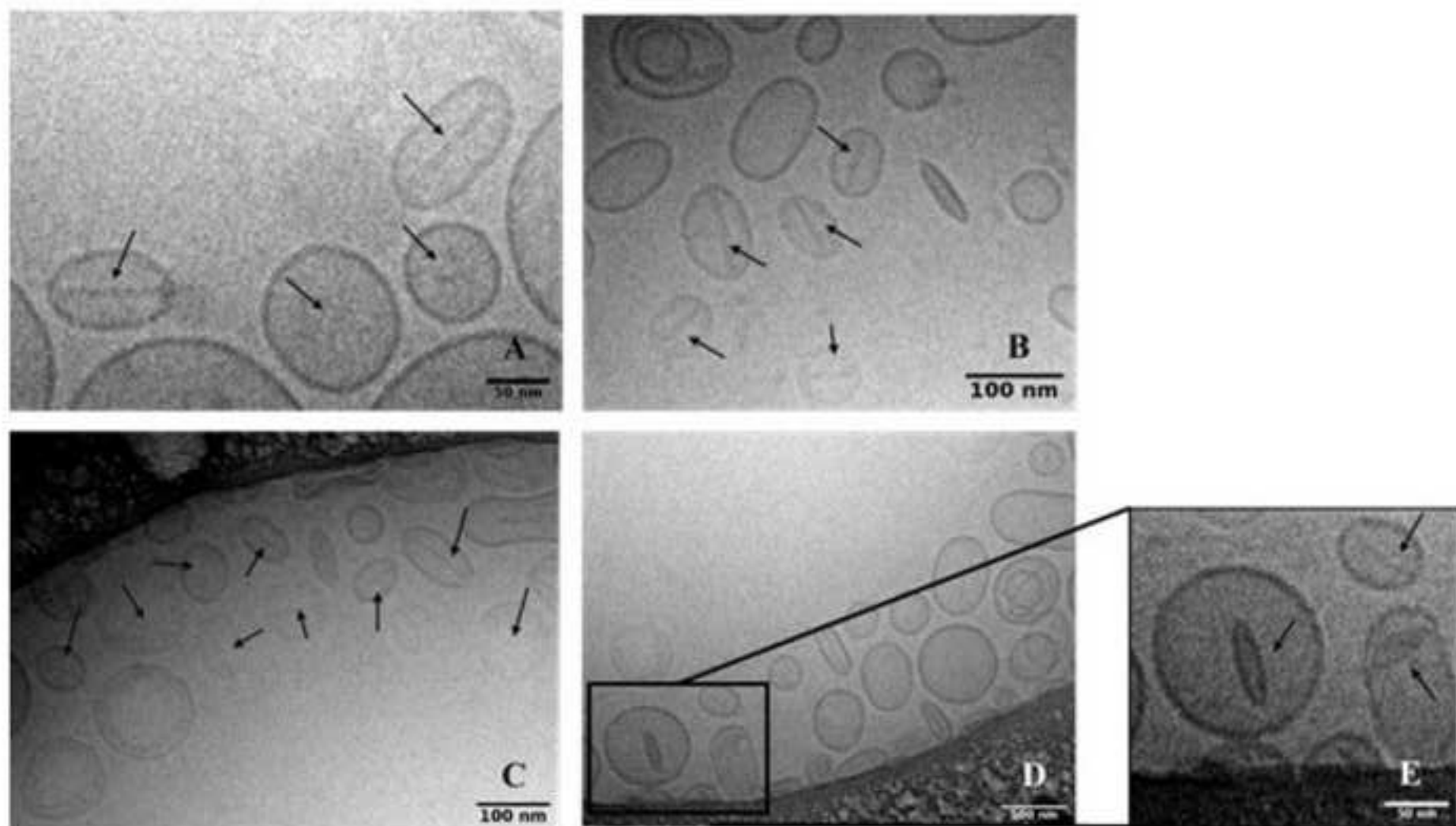


Figure 3

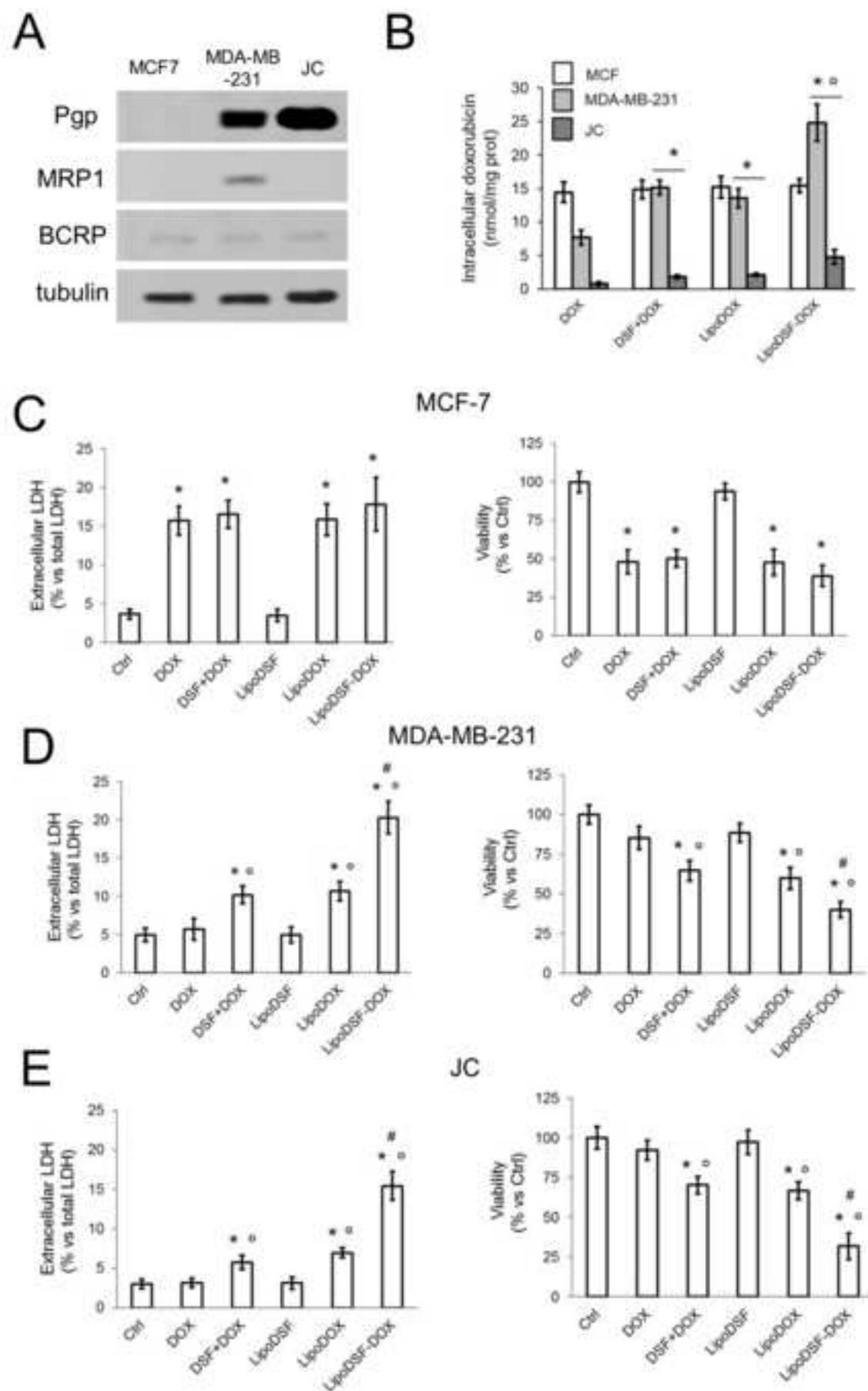


Figure 4

